

Conference materials

UDC 537.622.6

DOI: <https://doi.org/10.18721/JPM.161.161>

## Nanoscale layers of hexaferrite $\text{BaFe}_{12}\text{O}_{19}$ grown by laser molecular beam epitaxy: growth, crystal structure and magnetic properties

B.B. Krichevtsov <sup>1</sup>✉, A.M. Korovin <sup>1</sup>, S.M. Suturin <sup>1</sup>, N.S. Sokolov <sup>1</sup>

<sup>1</sup>Ioffe Institute, Saint Petersburg, Russia

✉ [boris@mail.ioffe.ru](mailto:boris@mail.ioffe.ru)

**Abstract.** Single-crystal 50 and 300 nm thick layers of BaM hexaferrite  $\text{BaFe}_{12}\text{O}_{19}$  were synthesized by laser molecular beam epitaxy method on  $\alpha\text{-Al}_2\text{O}_3$  (0001) substrates. Crystallization process was monitored *in situ* by RHEED and crystal structure was analyzed using three-dimensional mapping of diffraction patterns. The film surface morphology was investigated by atomic force microscopy. It was shown that the “as grown” structures exhibit hexaferrite structure but reveal violation of the long-range order, which is highly improved by the post growth annealing. Magnetic properties were studied by magneto-optical polar Kerr effect. Both the “as grown” and annealed structures were examined. After annealing, BaM hexaferrite films demonstrate square-type out-of-plane magnetic hysteresis loops indicating the presence of strong uniaxial magnetic anisotropy and remarkable pinning of domain walls.

**Keywords:** hexaferrite, molecular beam epitaxy, RHEED, atomic force microscopy, magneto-optical Kerr effect, magnetic properties

**Funding:** This study was funded by the Russian Science Foundation grant No. 22-22-00768, <https://rscf.ru/project/22-22-00768/>.

**Citation:** Krichevtsov B.B., Korovin A.M., Suturin S.M., Sokolov N.S., Nanoscale layers of hexaferrite  $\text{BaFe}_{12}\text{O}_{19}$  grown by laser molecular beam epitaxy: growth, crystal structure and magnetic properties, St. Petersburg State Polytechnical University Journal. Physics and Mathematics. 16 (1.1) (2023) 363–368. DOI: <https://doi.org/10.18721/JPM.161.161>

This is an open access article under the CC BY-NC 4.0 license (<https://creativecommons.org/licenses/by-nc/4.0/>)

Материалы конференции

УДК 537.622.6

DOI: <https://doi.org/10.18721/JPM.161.161>

## Наноразмерные слои гексаферрита $\text{BaFe}_{12}\text{O}_{19}$ , выращенные методом лазерной молекулярно-лучевой эпитаксии: рост, кристаллическая структура и магнитные свойства

Б.Б. Кричевцов <sup>1</sup>✉, А.М. Коровин <sup>1</sup>, С.М. Сутурин <sup>1</sup>, Н.С. Соколов <sup>1</sup>

<sup>1</sup>Физико-технический институт им. А.Ф. Иоффе РАН, Санкт-Петербург, Россия

✉ [boris@mail.ioffe.ru](mailto:boris@mail.ioffe.ru)

**Аннотация.** Монокристаллические слои гексаферрита BaM  $\text{BaFe}_{12}\text{O}_{19}$  толщиной 50 и 300 нм синтезированы методом лазерной молекулярно-лучевой эпитаксии на подложках  $\alpha\text{-Al}_2\text{O}_3$  (0001). Исследованы кристаллическая структура, морфология поверхности и магнитные свойства как “as grown”, так и отожженных структур.

**Ключевые слова:** гексаферрит, молекулярно-лучевая эпитаксия, ДБЭ, атомно-силовая микроскопия, магнитооптический эффект Керра, магнитные свойства

**Финансирование:** Работа выполнена при поддержке РФФ грант № 22-22-00768, <https://rscf.ru/project/22-22-00768/>.

**Ссылка при цитировании:** Кричевцов Б.Б., Коровин А.М., Сутурин С.М., Соколов Н.С. Наноразмерные слои гексаферрита  $\text{BaFe}_{12}\text{O}_{19}$ , выращенные методом лазерной

молекулярно-лучевой эпитаксии: рост, кристаллическая структура и магнитные свойства  
 // Научно-технические ведомости СПбГПУ. Физико-математические науки. 2023. Т. 16.  
 № 1.1. С. 363–368. DOI: <https://doi.org/10.18721/JPM.161.161>

Статья открытого доступа, распространяемая по лицензии CC BY-NC 4.0 (<https://creativecommons.org/licenses/by-nc/4.0/>)

## Introduction

One of the fundamental limitations hindering the development of modern element base for information processing is the release of Joule heat during the transport of charge carriers. A possible way to solve this problem is a utilization of magnonic devices based on the use of spin waves packets propagating in magnetic nanoheterostructures [1–3]. In this regard, the problem of creating thin film materials in which it is possible to excite, control, and record weakly damping spin waves arises. For these purposes, intensive studies of nanostructures based on garnet ferrites [4–7], spinel ferrites [8–11], and orthoferrites [11–14] were carried out.

Promising for microwave applications are M-type hexaferrites, a typical representative of which is  $\text{BaFe}_{12}\text{O}_{19}$  (BaM hexaferrite). The review of synthesis, properties and applications of hexaferrites can be found in Ref. [15]. Compared with the mentioned above magnetic garnets, spinels and orthoferrites, the hexaferrites have a number of advantages. Magnetization of BaM hexaferrite at  $RT$   $4\pi M_s \sim 4\text{ T}$  is higher than in yttrium iron garnet (YIG)  $4\pi M_s \sim 1.7\text{ T}$  and nickel ferrite (NFO)  $4\pi M_s \sim 3.3\text{ T}$ . The uniaxial magnetic anisotropy field  $H_a$  in BaM hexaferrite is about 1.75 T, that is two orders of magnitude higher than in YIG and one order higher than that of NFO. Due to high value of  $H_a$  the ferromagnetic resonance frequency in BaM hexaferrite  $f = \gamma(H + H_a - 4\pi M_s)$ , in the absence of an external field  $H = 0$  is about  $f \sim 36\text{ GHz}$  and linearly increases with external magnetic field  $H$ . As a result, devices based on hexaferrites can operate at frequencies up to  $f = 60\text{ GHz}$ . Moreover, textured polycrystalline hexaferrites can be created with a significant residual magnetization, which in some cases makes it possible to avoid the use of external magnets.

Thin films of hexaferrites were fabricated by liquid-phase epitaxy (LPE), pulsed laser deposition (PLD), direct current magnetron sputtering, screen printing (SP), and a metallo-organic decomposition (MO) methods on different substrates (sapphire,  $\text{Al}_2\text{O}_3$ , MgO, GdGa-garnet GGG, 6H-SiC). Comparison of films prepared by different methods, presented in [16], shows that the films of high crystal quality, prepared by PLD or LPE, show an out-of-plane orientation of c-axis and small values of FMR lines widths ( $\sim 30\text{--}60\text{ Oe}$ ) but also small values of remanence  $M_r$  for out-of-plane hysteresis loops. For this reason, for the application of these films in microwave devices an external magnetic field is needed. Contrary to that the films of lower crystal quality, fabricated by SP [17] or MO [18], have high hysteresis loop squareness ( $M_r/M_s \sim 0.9$ ), showing realization of self-bias effect, but large values of FMR line width. So, an obtaining a hexaferrite films with high crystal quality and high self-bias values is very desirable. Note that epitaxial films of BaM hexaferrite with in-plane orientation of easy axis and “self-bias” effect were synthesized by direct current magnetron sputtering on  $\alpha$ -plane (11-20) of single-crystal sapphire substrates [19].

This paper reports on the growth of single-crystalline layers of hexaferrite ( $\text{BaFe}_{12}\text{O}_{19}$ ) by laser molecular beam epitaxy on sapphire  $\alpha\text{-Al}_2\text{O}_3$  (0001) substrates and the study of their structural and magnetic properties.

## Materials and Methods

Thin films (thickness  $d \sim 50\text{ nm}$  and  $300\text{ nm}$ ) were grown using laser molecular beam epitaxy (MBE) method on  $\alpha\text{-Al}_2\text{O}_3$  (0001) substrates with an installation produced by “Surface, GmbH”. The films were grown in an oxygen atmosphere at a pressure of  $P = 0.04\text{--}0.06\text{ mBar}$  at growth temperatures of  $T_{\text{gr}} = 750\text{--}1000\text{ }^\circ\text{C}$ . The flow of matter onto the substrate was created by ablation of a stoichiometric  $\text{BaFe}_{12}\text{O}_{19}$  (Ba-hexaferrite M-type) target by a KrF excimer laser with a wavelength of 248 nm. The growth process was continuously monitored by reflection high-energy electron diffraction (RHEED). To analyze the RHEED patterns, the method of three-

dimensional mapping of diffraction patterns was applied. As a result of  $\varphi$ - $2\varphi$  scanning with a step of 0.01 degrees in  $\varphi$ , a series of 900 images was measured, from which a 3D map of the reciprocal space was obtained using the software. For our study we used both the as-grown structures and structures after annealing procedure. For post growth annealing, after preparation the samples were removed from the growth chamber and annealed up to 2 hours in air at the temperature of 1000 °C. Table 1 shows some parameters of presented in this work structures.

Table 1

**Sample number, thickness of hexaferrite layer, growth temperature  $T_{gr}$ , oxygen pressure  $P$ , annealing time  $t_{ann}$ , and annealing temperature  $T_{ann}$  of presented in this work BaM hexaferrite structures**

| Sample, № | Thickness, nm | $T_{gr}$ , °C | Oxygen pressure $P$ , mBar | Annealing time, min., and $T_{ann}$ , °C |
|-----------|---------------|---------------|----------------------------|--|
| 8940A     | 50            | 850           | 0.004                      | No                                       |
| 8940B     | 50            | 850           | 0.004                      | 120, 1000                                |
| 8944      | 50            | 950           | 0.06                       | No                                       |
| 8947      | 50            | 1000          | 0.06                       | No                                       |
| 8948A     | 50            | 750           | 0.06                       | No                                       |
| 8948B     | 50            | 750           | 0.06                       | 10, 1000                                 |
| 8948B+    | 50            | 750           | 0.06                       | 20, 1000                                 |
| 8948C     | 50            | 750           | 0.06                       | 60, 1000                                 |
| 8948C+    | 50            | 750           | 0.06                       | 120, 1000                                |
| 8949      | 50            | 925           | 0.06                       | No                                       |
| 8954A     | 300           | 750           | 0.06                       | No                                       |
| 8954B     | 300           | 750           | 0.06                       | 60, 1000                                 |

Magnetic hysteresis loops for out-of-plane orientation of magnetic field  $H$  (up to  $\pm 20$  kOe) were studied using magneto-optical polar Kerr effect by measuring the polarization plane rotation  $\phi$  of linearly polarized light ( $\lambda = 405$  nm) practically normally reflected from the film surface. Polarization modulation with Faraday cell was used to increase the measurements sensitivity ( $\delta\phi \sim 1$  sec. of arc).

## Results and Discussion

BaM hexaferrite layers grown at temperatures of 700–850 °C show RHEED images corresponding well to the bulk-BaM structure (Fig. 1, left). However, the enlarged width of the streaks and chaotic distribution of the streak intensity in these patterns indicate relatively low crystalline quality of the grown films. It is also seen that every second streak has a much higher intensity, which indicates a strong violation of the long-range order. In addition, it is worth noting that the RHEED patterns do not strongly depend on the  $O_2$  pressure in the range of 0.005–0.05 mbar.

In contrast to that, the films grown at 700–850 °C and then annealed in air at 1000 °C show the RHEED images perfectly modeled by the bulk BaM lattice (Fig. 1, center). It can be seen that the number of reflections and the signal-to-background ratio are much better compared to the non-annealed samples. All streaks have the same intensity, which indicates the presence of good long-range order.

It was found that the samples grown at temperatures of 900–1000 °C are very different as compared to those grown at lower temperatures. RHEED patterns from such samples are well modeled by the  $\alpha$ - $Fe_2O_3$  lattice (Fig. 1, right). The formation of  $\alpha$ - $Fe_2O_3$  is most likely associated with resputtering (desorption induced by impinging particles) of Ba ions at high temperatures. The account of resputtering process can explain the effect of 1000 °C annealing on crystal quality of films grown at low temperatures. In films grown at  $T_{gr} = 700$ –850 °C the resputtering is small and Ba ions are distributed more or less homogeneously inside of hexaferrite film. The annealing results in redistribution of Ba positions and occupation by Ba ions of places corresponding to BaM crystal structure that leads to formation of high crystal quality BaM layer with improved magnetic properties (see below). The growth of films at 1000 °C is followed to disappearance of

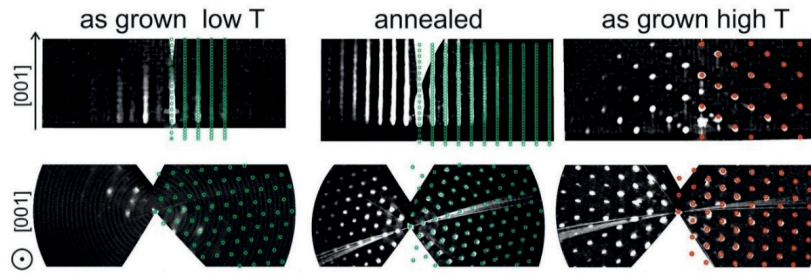


Fig. 1. 3D reconstruction of RHEED data for BaM films N8954A grown at 800 °C (left), N8954B grown at 800 °C and annealed for 1 hour at 1000 °C (center) and N 8947 grown at 1000 °C (right) in the same scale; green and red dots are a model lattice calculated using parameters of bulk BaM crystal. Films in left and central panels have thickness ~ 300 nm and in left panel ~ 50 nm

Ba ions from film and to formation of  $\alpha$ -Fe<sub>2</sub>O<sub>3</sub> structure.

Most of “as-grown” BaM films do not reveal any hysteresis magnetic loops in out-of-plane magnetic field. Only structures N 8944 and 8949 grown at  $T_{gr} = 950$  and  $925$  °C shows small and wide ( $H_c \sim 7$  kOe) hysteresis loops (Fig.2, a).

Annealing leads to a sharp change in the hysteresis loops. Fig 2, b illustrates this fact on example of the “as grown” (N 8940A) and annealed (N 8940B) at 1000 °C during 120 min parts of the same film. After annealing, an almost rectangular loop ( $M_r/M_s \sim 1$ ,  $M_r$  and  $M_s$  are remnant and saturated magnetization correspondingly) is observed with a coercive field  $H_c = 2.5$  kOe. The effect of annealing on the magnetic properties of the films was observed in all structures grown at  $T_{gr} = 700$ – $850$  °C. The effect of annealing time  $t_{ann}$  on shape of hysteresis loops is presented in Fig.2, c. Even 10 minutes annealing results in the appearance of a hysteresis loop. An increase of  $t_{ann}$  leads to an increase of both the magnitude of PMOKE in saturation and  $M_r/M_s$  ratio (Fig. 2, d), but does not change the coercive field value  $H_c = 2.5$  kOe. The jumps in the magnetization at  $H = \pm H_c$  are obviously caused by the formation of domains with the opposite orientation of the magnetization and the motion of the domain walls.

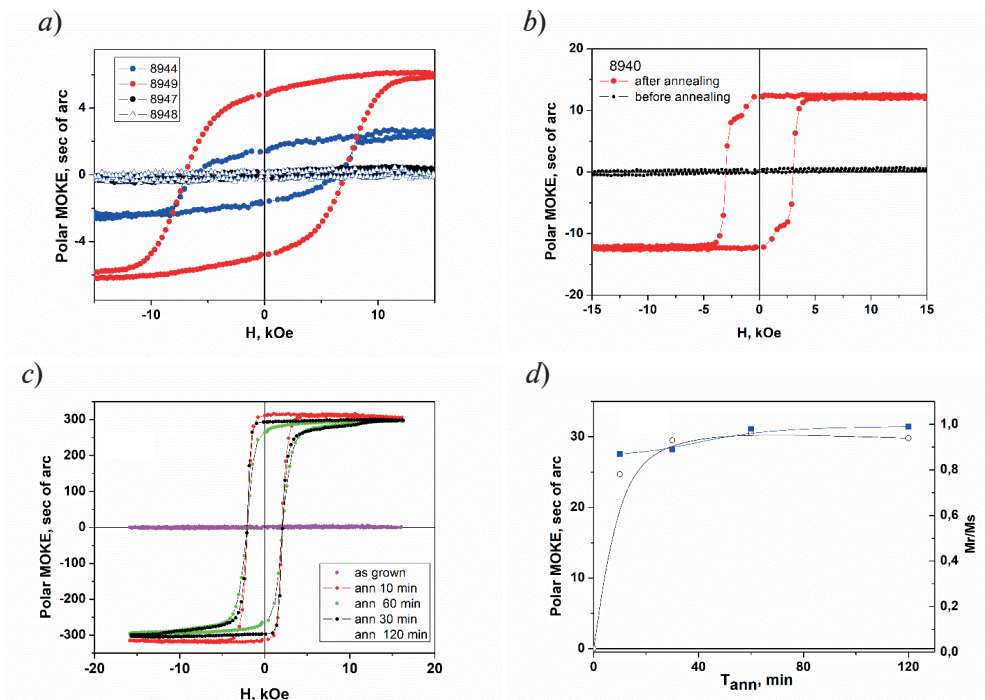


Fig. 2. Magnetic hysteresis loops measured by MOKE in “as grown” films N 8944, 8947, 4948, 8949 (a). Effect of 120 min 1000 °C annealing in 8940 film (b). Effect of annealing time  $t_{ann}$  on hysteresis loops in film N 8948 (c, d)





Relatively high values of  $H_c$  in our structures indicate that domains in BaM layers are pinned on defects in contrast to films prepared in [16].

### Conclusion

The study showed that thin layers of BaM hexaferrite obtained by laser molecular beam epitaxy on sapphire (0001) substrates demonstrate well-ordered BaM crystal structure after post-growth annealing in air at 1000 °C of the samples grown at  $T_{gr} = 700–850$  °C. The observation of rectangular loops in the fabricated BaM structures indicates the presence of a strong out-of-plane uniaxial magnetic anisotropy, which makes it possible to realize a saturated magnetic state with an out-of-plane orientation of magnetization in the absence of an external magnetic field  $H$ . This may be of interest for the creation of UHF microwave devices that use bulk spin waves for the operation. Future studies of these structures will focus on XRD crystal structure measurements, VSM magnetization studies, and FMR spectroscopy.

### Acknowledgments

Authors thank Dr. K. Mashkov for help with carrying out MOKE experiments.

### REFERENCES

1. Kruglyak V.V., Demokritov S.O., Grundler D., *Magnonics*, J. Phys. D. Appl. Phys. 43 (2010) 264001 (14pp).
2. Nikitov S.A., Kalyabin D.V., Lisenkov I.V., Slavin A.N., Barabanenkov Yu.N., Osokin S.A., Sadovnikov A.V., Beginin E.N., Morozova M.A., Sharaevsky Yu.P., Filimonov Yu.A., Khivintsev Yu.V., Vysotsky S.L., Sakharov V.K., Pavlova E.S., *Magnonics: a new research area in spintronics and spin wave electronics*, Physics-Uspekhi. 58 (2015) 1002–1028.
3. Grundler D., *Nanomagnonocs*, J. Phys. D. Appl. Phys. 49 (2016) 2014–2017.
4. Serga A.A., Chumak A.V., Hillebrands B., *YIG magnonocs*, J. Phys. D. Appl. Phys. 43 (2010) 264002.
5. Howe B.M., Emori S., Jeon H., Oxholm T.M., Jones J.G., Mahalingam K., Zhuang Y., Sun N.X., Brown G.J., *Pseudomorphic Yttrium Iron Garnet Thin Films with Low Damping and Inhomogeneous Linewidth Broadening*, IEEE Magn. Lett. 6 (2015), 2013–2016.
6. Sokolov N.S., Fedorov V.V., Korovin A.M., Suturin S.M., Baranov D.A., Gastev S.V., Krichevtsov B.B., Maksimova K.Yu., Grunin A.I., Bursian V.E., Lutsev L.V., Tabuchi M., *Thin yttrium iron garnet films grown by pulsed laser deposition: Crystal structure, static, and dynamic magnetic properties*, J. Appl. Phys., 119 (2016) 023903.
7. Chang H., Li P., Zhang W., Liu T., Hoffmann A., Deng L., Wu M., *Thin yttrium iron garnet films grown by pulsed laser deposition: Crystal structure, static, and dynamic magnetic properties*, IEEE Magn. Lett. 5 (2014) 10–13.
8. Chinnasamy C.N., Yoon S.D., Yang A., Baraskar A., Vittoria C., Harris V. G., *Effect of growth temperature on the magnetic, microwave, and cation inversion properties on NiFe<sub>2</sub>O<sub>4</sub> thin films deposited by pulsed laser ablation deposition*, J. Appl. Phys. 101 (2007) 09M517.
9. Singh A. V., Khodadadi B., Mohammadi J.B., Keshavarz S., Mewes T, Negi D.S., Ranjan Datta, Galazka Z., Uecker R., Gupta A., *Bulk Single Crystal-Like Structural and Magnetic Characteristics of Epitaxial Spinel Ferrite Thin Films with Elimination of Antiphase Boundaries*, Adv. Mater. 29 (2017) 1701222.
10. Krichevtsov B., Gastev S., Mashkov K., Kaveev A., Korovin A., Lutsev L., Suturin S., Lobov I., Telegin A., Lomov A. Sokolov N., *Magnetization reversal in NiFe<sub>2</sub>O<sub>4</sub>/SrTiO<sub>3</sub> nanoheterostructures grown by laser molecular beam epitaxy*, J. Phys. Conf. Ser. 1389 (2019), 012106.
11. Bursian V.E., Kaveev A.R., Alexander, Korovin A.M., Krichevtsov B.B., Lutsev L.V., Suturin S.M., Sawada M., Sokolov N.S., *Bulk-Like Dynamic Magnetic Properties of Nickel Ferrite Epitaxial Thin Films Grown on SrTiO<sub>3</sub>(001) Substrates*, IEEE Magn. Lett. 10 (2019) 6104505.
12. Ning S., Kumar A., Klyukin K., Cho E., Kim J. H., Su T., Kim H.-S., LeBeau J.M., Bilge Yildiz B., Ross C.A., *An antisite defect mechanism for room temperature ferroelectricity in orthoferrites*, Nature Communications. (2021) 12:4298.
13. Jeong Y.K. , Lee J.-H., Ahn S.-J., Song S.-W., Jang H.M., Choi H., Scott J.F., *Structurally*

Tailored Hexagonal Ferroelectricity and Multiferroism in Epitaxial YbFeO<sub>3</sub> Thin-Film Heterostructures, J. Am. Chem.Soc. 134 (2012) 1450–1453.

14. **Seo J.W., Fullerton E.E., Nolting F., Scholl A., Fompeyrine J., Locquet J-P.**, Antiferromagnetic LaFeO<sub>3</sub> thin films and their effect on exchange bias, J. Phys.: Condens. Matter. 20 (2008) 264014.

15. **Pullar R.C.**, Progress in Materials Science. 57 (2012) 1191–1334.

16. **Su Z., Bennett S., Hu B., Yajie Chen Y., Harris V.G.** Magnetic and microwave properties of U-type hexaferrite films with high remanence and low ferromagnetic resonance linewidth, J. Appl. Phys. 99 (2006) 08M911.

17. **Nie Y., Harward I., Balin K., Beaubien A., Celinski Z.**, Preparation and characterization of barium hexagonal ferrite thin films on a Pt template, J. Appl. Phys. 107 (2010) 073903.

18. **Chen Y., Sakai T., Chen T., Yoon S.D., Geiler A.L., Vittoria C., Harris V.G.** Appl. Phys. Lett 88 (2006) 062516.

19. **Zhang X., Meng S., Song D., Zhang Y., Yue Zh., Harris V.G.**, Epitaxially grown BaM hexaferrite films having uniaxial axis in the film plane for self-biased devices, Sci. Rep. 7 (2017) 44193.

### THE AUTHORS

**KRICHEVTSOV Boris B.**

boris@mail.ioffe.ru

ORCID: 0000-0003-4032-8708

**SUTURIN Sergey M.**

Suturin@mail.ioffe.ru

ORCID: 0000-0002-3662-2384

**KOROVIN Alexander M.**

Amkorovin@mail.ioffe.ru

ORCID: 0000-0002-3255-9808

**SOKOLOV Nikolai S.**

Nsokolov@fl.ioffe.ru

ORCID: 0000-0002-8763-3489

*Received 24.10.2022. Approved after reviewing 09.11.2022. Accepted 15.11.2022.*